Coupled Geomechanical CFD Modelling of Goaf under Goaf Gas Drainage: Impact of Goaf Characteristics

Yuehan Wang
School of Minerals and Energy Resources Engineering, University of New South Wales, Sydney, Australia

Guangyao Si
School of Minerals and Energy Resources Engineering, University of New South Wales, Sydney, Australia

Joung Oh
School of Minerals and Energy Resources Engineering, University of New South Wales, Sydney, Australia

ABSTRACT: Australian mines heavily relied on a series of boreholes to control goaf gas emissions. The use of these boreholes not only reduces greenhouse gas but also recovers a large amount of energy. However, high suction pressure applied on boreholes may cause ventilation air migration from the working face to enter the goaf. The leaked air containing rich oxygen would react with the residual coal in the goaf and accumulate heat, which may cause spontaneous combustion and gas explosion risks. This paper developed a goaf CFD model to analyse the goaf gas distribution and leaked air flow pathways under the impact of intensive goaf gas drainage. Besides, the associated gas explosion risks will be quantified using Coward's triangle based on the CFD modelling simulation results. Therefore, this CFD model can be used to optimise the drainage efficiency of intensive boreholes while ensuring mining safety during the operation period.

Keywords: Goaf gas drainage, CFD modelling, goaf permeability, coal oxidation, gas explosion risk.

1 INTRODUCTION

Goaf gas drainage is crucial in Australian coal mines to control high gas emissions from the longwall goaf. This method involves drilling vertical boreholes from the surface to extract gas emissions from the goaf and maintain methane levels in working areas at safe levels. Goaf gas drainage does not interrupt production and captures high-purity gas from multiple coal seams. However, it has raised concerns about oxygen-rich ventilation air being drawn back into the goaf, increasing the goaf explosion and sponcom risks. To improve efficiency and mining safety, understanding gas migration mechanisms in the longwall goaf and the impact of various factors on the goaf environment is necessary.

With the advancement of computer calculation efficiency, computational fluid dynamics (CFD) modelling has been developed to understand goaf gas behaviours and gas flow patterns (e.g. Balusu et al. 2002, Balusu et al. 2004, Ren & Balusu 2005, Ren & Balusu 2009, Yuan & Smith 2008 and 2010, Brune 2013). The CFD results revealed that air leakage into the goaf area is mainly from the maingate, and the goaf caving follows an 'O-shaped' or 'annular-shaped' compaction trend (e.g. Qian & Xu 1998 and Guo et al. 2012). The O_2 distribution in a conventional goaf gas CFD model

shows a higher concentration and travels farther away from the face into the goaf at the maingate side, compared with that on the tailgate side (e.g., Balusu et al. 2002 and Balusu et al. 2004). Some models also showed that the CH4 concentration increases with the distance away from the working face due to gas desorption from residual coal and migration from adjacent strata (e.g., Balusu et al 2004 and Guo et al. 2015). Moreover, CFD modelling has been used to assess the risk of goaf explosions in coal mines. Some researchers used CFD modelling to investigate the impact of different factors on the goaf explosion risks, which include mining conditions, coal seam gas content, and ventilation scenarios. These studies suggest reducing mining speed (Li et al. 2016), improving gas drainage systems and coal seam degasification (Xia et al. 2016), increasing ventilation rates and using barrier curtains (Zhang et al. 2020) to mitigate the explosion risk. However, there is currently no CFD model based on substantial field measurement data that can consider both coal seam gas flow and self-heating in the goaf.

Therefore, it is imperative to investigate how intensive goaf gas drainage would affect the goaf environment, especially oxygen migration pathways. When calibrating the CFD models to simulate goaf gas flow, different natural characteristics of the goaf will also be considered, such as gas emission rate, permeability change, and goaf ventilation, to understand the sensitivity of various factors to affect the goaf atmosphere.

2 MODELLING GOVERNING EQUATIONS

This paper used FLUENT, one of the more mature commercial CFD software packages, to build the goaf CFD modelling. It employs the Navier-Stokes equation to describes the motion of fluids in terms of their density, velocity, and pressure. The chemical reactions between coal and oxygen at low temperatures are complex and dependent on various internal and external factors. The simplified chemical reaction between coal and oxygen used in this paper is displayed as the following Equation 1 (e.g. Yuan & Smith 2008 and 2009).

$$\mathrm{Coal} + \mathrm{O_2} \rightarrow \mathrm{CO_2} + 0.1\mathrm{CO} + \mathrm{Heat} \tag{1}$$

The heat of reaction is computed utilising the heat of formation of the reactants (coal) and the products (CO_2 and CO), applied in the CFD model using the UDF code. In order to mathematically define the oxidation reaction rate r of coal, the Arrhenius reaction mechanism typically employs the relationship between the reaction oxidation rate r and the temperature and oxygen concentration.

$$\mathrm{r} = \mathrm{A}[\mathrm{O_2}]^{\mathrm{n}}\exp(-\frac{\mathrm{E}}{\mathrm{RT}}) \tag{2}$$

Where r is the chemical reaction rate (kmol/(m^3s)); A is the pre-exponential factor ((kmol/m3)$^{(1-n)}$s^{-1}; $[O_2]$ is the oxygen concentration (kmol/m^3); n is the apparent order of reaction and n value in low-temperature oxidation studies of coal and other carbonaceous materials has been shown to vary from 0.5 to 1.0 (Smith & Lazzara, 1987); E is the apparent activation energy (kcal/mol); R is gas constant (kcal/mol K); T is the absolute temperature (K).

Based on the simplified coal oxidation reaction described above, the species conservation of oxygen, carbon dioxide and carbon monoxide are as follows:

For oxygen:

$$\varepsilon\frac{\partial(\rho\mathrm{C_{O_2}})}{\partial\mathrm{t}} + \varepsilon\nabla\left(\rho\vec{\mathrm{v}}\mathrm{C_{O_2}}\right) = \nabla\left(\rho\mathrm{D_{O_2}}\mathrm{C_{O_2}} + \mathrm{D_{T,O_2}}\frac{\nabla\mathrm{T}}{\mathrm{T}}\right) - \mathrm{r} \tag{3}$$

For carbon dioxide:

$$\varepsilon\frac{\partial(\rho\mathrm{C_{CO_2}})}{\partial\mathrm{t}} + \varepsilon\nabla\left(\rho\vec{\mathrm{v}}\mathrm{C_{CO_2}}\right) = \nabla\left(\rho\mathrm{D_{CO_2}}\mathrm{C_{CO_2}} + \mathrm{D_{T,CO_2}}\frac{\nabla\mathrm{T}}{\mathrm{T}}\right) + \mathrm{r} \tag{4}$$

For carbon monoxide:

$$\varepsilon\frac{\partial(\rho\mathrm{C_{CO}})}{\partial\mathrm{t}} + \varepsilon\nabla(\rho\vec{\mathrm{v}}\mathrm{C_{CO}}) = \nabla\left(\rho\mathrm{D_{CO}}\mathrm{C_{CO}} + \mathrm{D_{T,CO}}\frac{\nabla\mathrm{T}}{\mathrm{T}}\right) + 0.1\mathrm{r} \tag{5}$$

Where C_{O_2}, C_{CO_2} and C_{CO} are the mass fraction of oxygen, carbon dioxide and carbon monoxide, respectively; D_{O_2}, D_{CO_2} and D_{CO} are the effective mass diffusion coefficient of O_2, CO_2 and CO, respectively.

3 MODELLING DESCRIPTION

CFD models to simulate the goaf environment with boreholes are developed in three steps: pre-processing, solving, and post-processing. In this section, the goaf geometric model and the meshing are presented, as well as the related parameters setting in the solver-FLUENT.

3.1 Geometry & mesh modelling settings

Based on the case longwall panel (LWA) geometry and the U-shaped ventilation system, a simplified goaf geometry model with a width of 350 m and a length of about 1000 m was built in SpaceClaim, as illustrated in Figure 1. Besides, the depth of this geometry model is 22.5 m. There are eight vertical boreholes (BH1 to BH8) with 250 mm diameter situated 30 m from the goaf TG side, with the bottoms 10 m from target coal seams. BH1 is 50 m from the working face, and adjacent boreholes are 50 m from one another. In addition, the cut-throughs (C/T) on the MG side are 120 m apart from one another. After the geometry model has been constructed, the Meshing module can be used to separate it into appropriate grids. In this study, the goaf area, bottom coal layer, and other elements of the geometry model are meshed using the cut-cell approach with different size controls. Figure 2 shows that boreholes have a mesh size of 0.05 m, and the final goaf zone is combined by the fine mesh (1.5 m) near the working face and the coarse mesh (5 m) further away.

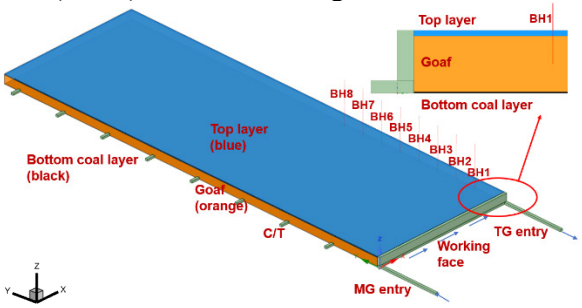

Figure 1. Goaf geometry model.

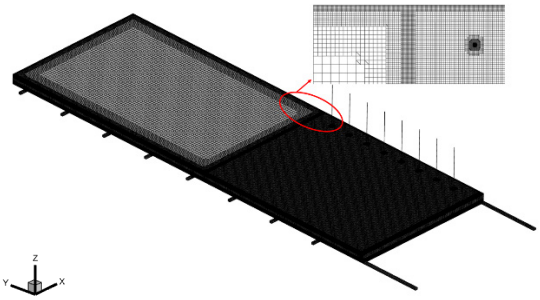

Figure 2. Goaf mesh model.

3.2 Goaf permeability & boundary conditions

Once the mesh was completed with high quality, it could be imported into FLUENT to be solved. This model is divided into the porous media domain (goaf and coal layer) and free flow domain (maingate, tailgate and working face). In the free flow domain, airflow is assumed to be completely turbulent, and the standard k-ε model is used to solve this model. The laminar flow zone option is enabled in the goaf and coal layer to suppress the turbulent viscosity of the fluid in the porous media domain. For the goaf and coal layer zone, the porosity and permeability will be applied to this CFD model via UDF codes, which are based on the history matching of field gas production data (e.g. Wang et al 2022a and 2022b) and empirical values in the literature review. In this model, the porosity change along the TG side goaf and MG side goaf was assumed to be equivalent, as shown in Figure 3.

Furthermore, this model has two fluid inlets: one for ventilation airflow and one for gas emissions from the goaf residual coal and adjacent strata. This ventilation airflow inlet at MG entry has a velocity magnitude of 2.2 m/s and provides 60 m^3/s of air to the longwall working face, which contains 20.9% oxygen. In addition, the gas emission is simplified in this model as a velocity inlet distributed throughout the top layer. Figure 4 shows the defined gas emission trend per square meter of the top layer, which varies with the distance from the working face. Regarding fluid outlets, apart from the TG entry as one outlet, there are -6500 kPa suction pressures applied at the top surface of each vertical borehole to extract the goaf gas.

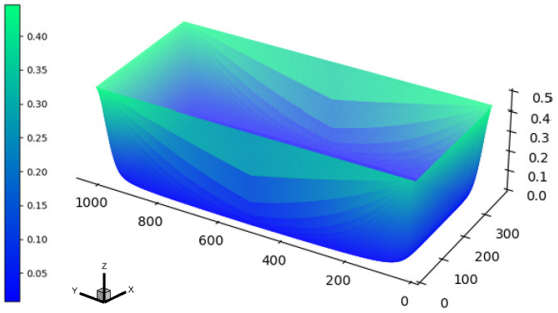

Figure 3. Goaf porosity distribution.

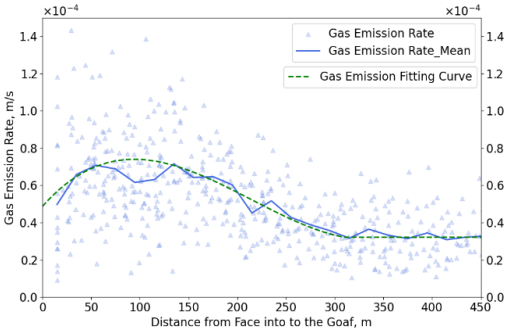

Figure 4. Gas emission trend for velocity-inlet.

4 MODELLING RESULTS

4.1 Goaf gas distributions

Figure 5 (a) below shows the oxygen contour distribution in the goaf (at the level of 10 m above the seam, i.e., the borehole completion depth) under the drainage impact of eight active boreholes. It is clear that the implementation of continuous goaf drainage has resulted in an oxygen-rich zone on the TG side goaf. The size of this oxygen-rich zone depends on the location of boreholes. Figure 6 (a) shows the goaf oxygen profiles along the two dashed lines in Figure 5 (a). The oxygen concentration in drained boreholes is also shown in green triangular dots. At the MG side, a sharp decline can be observed in the O_2 profile, which reduces to almost 0% at 50 m away from the face. However, the O_2 level at the TG side is reported to be much higher, due to the strong suction pressure applied by the nearby boreholes. It is also interesting to observe that the O_2 concentration reported in boreholes (Figures 6 (a) & 7 (a)) is much lower than that in the goaf reservoir near the borehole. This is reasonable as boreholes would preferentially drain CH_4 emitted from the top layer. This suggests the actual O_2 concentration in the goaf atmosphere would be much higher than that observed in the drained gas from boreholes.

Due to the sweep of ventilation air at the face, the CH_4 level is quite low near the face and slowly increases in the deep goaf (Figure 5 (b)). As Figure 6 (b) shows, the TG side goaf has much lower CH_4 compared with that on the MG side since goaf drainage has drawn a large amount of air into the TG side goaf. The CH_4 purity found in boreholes (as indicated by the green triangular dots) is also much higher than that in the goaf reservoir, which is consistent with the field data results (Figure 7 (b)). Besides, as shown in Figure 5 (c), more CO production was also observed on the goaf TG side as the boreholes drive more oxygen into deeper goaf. Eventually, the CO content extracted from the boreholes reached a maximum value of approximately 40 ppm at 100 m (BH2), which is consistent with the magnitude of the field data (Figure 7(c)).

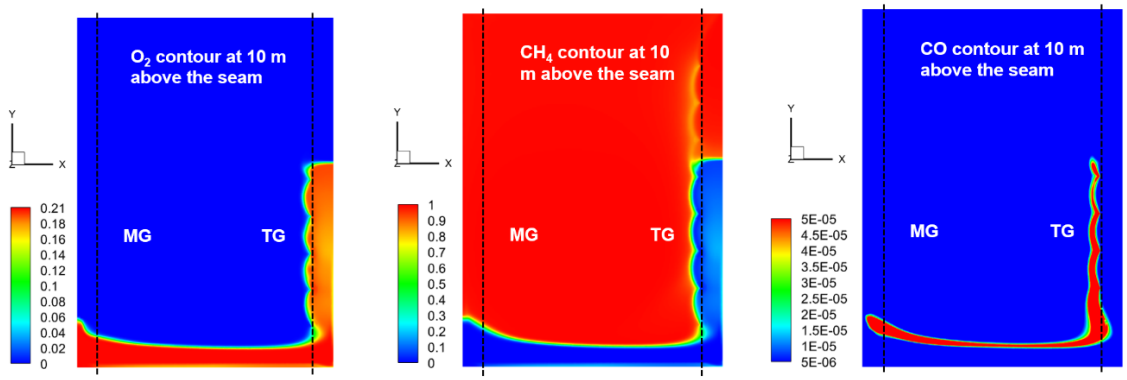

(a) (b) (c)

Figure 5. Goaf gas distribution in the goaf at 10 m above the seam: (a) O_2, (b) CH_4 and (c) CO.

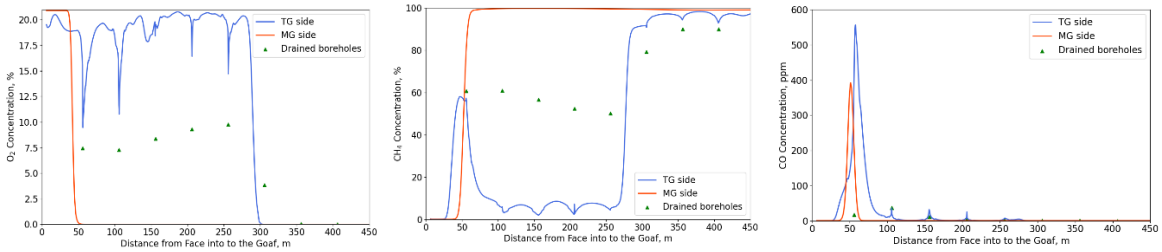

(a) (b) (c)

Figure 6. Goaf gas profiles along the two dashed lines: (a) O_2, (b) CH_4 and (c) CO.

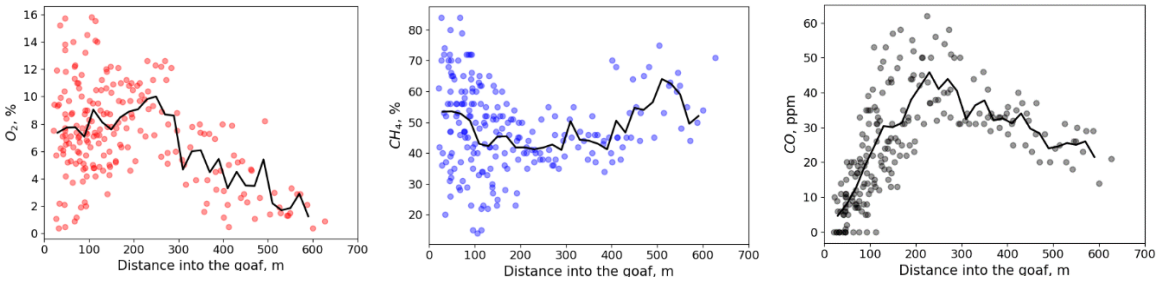

(a) (b) (c)

Figure 7. Goaf gas profiles along TG side from the field data (a) O_2, (b) CH_4 and (c) CO (Si & Belle 2019).

4.2 Goaf explosion risk assessment

The Coward triangle is usually used to assess the gas explosion risk, which has been proven effective in indicating a gas mixture's explosibility (Coward & Jones 1952). The gas explosion risk in this study can be quantified by combining the O_2 and CH_4 concentration results from the CFD modelling with the Coward triangle. As a result, the explosion zone at 10 m above the seam cut-off is displayed in Figure 8. There are four distinct regions in Figure 8: the explosive zone (red), the fuel-rich zone that can become explosive when fresh air or oxygen is added (yellow), the fuel-lean zone that can become explosive when fuel is added (blue), and the non-explosive zone where no explosive composition is possible (green). Different coloured zones of the Coward triangle illustrate the explosive potential for the mixtures of methane and air. The explosion zone (red) in this diagram illustrates the migration of the explosion zone away from the working face under the influence of goaf gas drainage. The temperature change after coal reaction is shown in Fig. 8(b), compared with the initial temperature setting of 300 K (27°C). Moreover, the sensitivity of different goaf natural characteristics (e.g., gas emission, ventilation system, goaf permeability) to the goaf environment, gas flow patterns, and potential explosion risks are also assessed in this study.

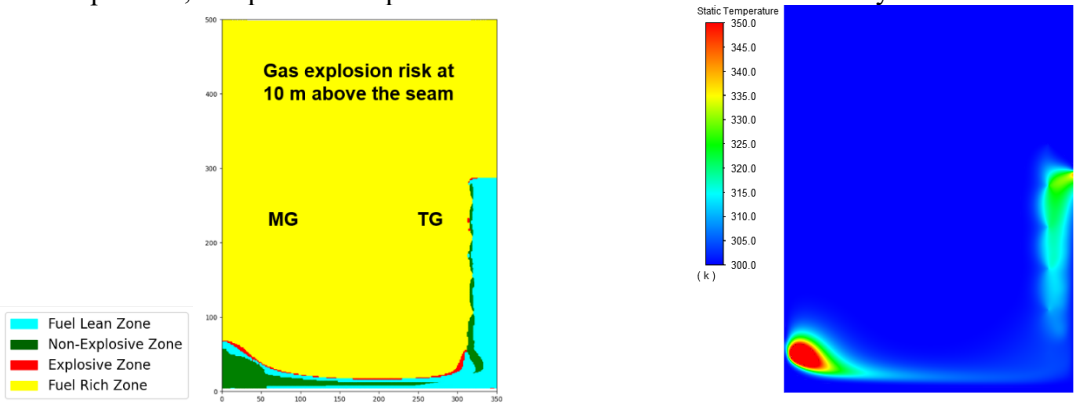

(a) (b)

Figure 8. (a) Goaf explosion zone and (b) temperature in the goaf at 10 m above the seam.

ACKNOWLEDGEMENTS

The authors would like to thank Australian Coal Association Research Program (ACARP) C29017 and C34011 for supporting this work. The authors would also like to thank Australian Research Council Linkage Program (LP200301404) for sponsoring this research.

REFERENCES

Balusu, R., Humphries, P., Harrington, P., Wendt, M., Xue, S. 2002. Optimum inertisation strategies. *In Proceedings of Queensland Mining Industry Health and Safety Conference*, Townsville, Australia, pp.133-144.

Balusu, R., Neil, R., Ron, P., Tim, H., Shen, Z. & Haruko, I. 2004. Optimisation of longwall goaf gas drainage & control system, ACARP report C10017.

Brune, J. F. 2013. CFD modeling of gas flow and spontaneous heating in longwall gob areas. In: *Proceedings of the 32nd International Conference on Ground Control in Mining*, pp. 124-133.

Coward, H. F., & Jones, G. W. 1952. Limits of flammability of gases and vapors. US Government Printing Office, pp. 503-508

Deng, J., Ma, X., Zhang, Y., Li, Y., & Zhu, W. 2015. Effects of pyrite on the spontaneous combustion of coal. International Journal of Coal Science & Technology, 2, pp. 306-311.

Guo, H., Yuan, L., Shen, B., Qu, Q. and Xue, J. 2012. Mining-induced strata stress changes, fractures and gas flow dynamics in multi-seam longwall mining. International Journal of Rock Mechanics and Mining Sciences, 54, pp.129–139.

Guo, H., Todhunter, C., Qu, Q., & Qin, Z. 2015. Longwall horizontal gas drainage through goaf pressure control. International Journal of Coal Geology, 150-151, pp.276-286.

Xia, T., Zhou, F., Wang, X., Zhang, Y., Li, Y., Kang, J., & Liu, J. 2016. Controlling factors of symbiotic disaster between coal gas and spontaneous combustion in longwall mining gobs. Fuel, 182, pp. 886-896.

Li, L., Li, D., Li, S., Liu, Y., & Yao, Y. 2016. Investigation of spontaneous combustion risk in the goaf with different mining speeds. *Safety Science* 84, pp. 197-206.

Qian, M., & Xu, J. 1998. Characteristics of air leakage in the longwall mining face and its control. *Journal of China Coal Society* 23(3), pp. 239-244.

Ren, T. & Balusu, R. 2005. CFD modelling of goaf gas migration to improve the control of spontaneous combustion in longwalls, *In: Coal Operators' Conference*, Wollongong, pp. 259–264.

Ren, T. & Balusu, R. 2009. Proactive goaf inertisation for controlling longwall goaf heatings. *Procedia Earth and Planetary Science*, 1 (1), pp. 309-315.

Si, G., & Belle, B. 2019. Performance analysis of vertical goaf gas drainage holes using gas indicators in Australian coal mines. *International Journal of Coal Geology* 216, pp. 103301.

Smith, A. C., & Lazzara, C. P. 1987. Spontaneous combustion studies of US coals. vol. 9079. US Department of the Interior, Bureau of Mines.

Wang, Y., Si, G., Xiang, Z., Oh, J., Belle, B., & Webb, D. 2022a. A theoretical goaf resistance model based on gas production analysis in goaf gas drainage. *International Journal of Coal Geology* 264, pp. 104140.

Wang, Y., Si, G., Belle, B., Oh, J. & Xiang, Z. 2022b. In: *AusIMM mine ventilation conference 2022*, Gold Coast, Australia, October 10-12, 2022, pp. 436-446.

Yuan, L., & Smith, A. C. 2008. Numerical study on effects of coal properties on spontaneous heating in longwall gob areas. Fuel, 87(15-16), 3409-3419.

Yuan, L., & Smith, A. C. 2009. CFD modelling of spontaneous heating in a large-scale coal chamber. *Journal of Loss Prevention in the Process Industries*, *22*(4), 426-433.

Zhang, J., An, J., Wen, Z., Zhang, K., Pan, R., & Al Mamun, N. A. 2020. Numerical investigation of coal self-heating in longwall goaf considering airflow leakage from mining induced crack. *Process Safety and Environmental Protection*, 134, pp. 353-370.